

# Semileptonic decays of $B(B_s)$ to light tensor mesons

R. Khosravi\*, S. Sadeghi

*Department of Physics, Isfahan University of Technology, Isfahan 84156-83111, Iran*

## Abstract

The semileptonic  $B_s(B) \rightarrow K_2^*(a_2, f_2)\ell\nu$ ,  $\ell = \tau, \mu$  transitions are investigated in the frame work of the three-point QCD sum rules. Considering the quark condensate contributions, the relevant form factors of these transitions are estimated. The branching ratios of these channel modes are also calculated at different values of the continuum thresholds of the tensor mesons and compared with the obtained data for other approaches.

PACS numbers: 11.55.Hx, 13.20.He, 14.40.Be

---

\* e-mail: rezakhosravi @ cc.iut.ac.ir

## I. INTRODUCTION

Investigation of the  $B$  meson decays into tensor mesons are useful in several aspects such as CP asymmetries, isospin symmetries and the longitudinal and transverse polarization fractions. A large isospin violation has already been experimentally detected in  $B \rightarrow \omega K_2^*(1430)$  mode [1]. Also, the decay mode  $B \rightarrow \phi K_2^*(1430)$  is mainly dominated by the longitudinal polarization [2, 3], in contrast with the  $B \rightarrow \phi K^*$  where the transverse polarization is comparable with the longitudinal one [4]. Therefore, nonleptonic and semileptonic decays of  $B$  meson can play an important role in the study of the particle physics.

In the flavor  $SU(3)$  symmetry, the light  $p$ -wave tensor mesons with  $J^P = 2^+$  containing iso-vector mesons  $a_2(1320)$ , iso-doublet states  $K_2^*(1430)$ , and two iso-singlet mesons  $f_2(1270)$  and  $f_2'(1525)$ , are building the ground state nonet which have been experimentally established [5, 6]. The quark content  $q\bar{q}$  for the iso-vector and iso-doublet tensor resonances are obvious. The iso-scalar tensor states,  $f_2(1270)$  and  $f_2'(1525)$  have a mixing wave functions where mixing angle should be small [7, 8]. Therefore,  $f_2(1270)$  is primarily a  $(u\bar{u} + d\bar{d})/\sqrt{2}$  state, while  $f_2'(1525)$  is dominantly  $s\bar{s}$  [9].

The semileptonic decays of  $B$  involving  $K(K^*, K_0^*)$  have been studied in the framework of the three-point QCD sum rules (3PSR), for instance  $B \rightarrow K\ell^+\ell^-$ ,  $B \rightarrow K^*\ell^+\ell^-$  [15],  $B_s \rightarrow K_0^*\ell\nu$  [16] and  $B_s \rightarrow (K_0^*, f_0)\ell^+\ell^-$  [17]. As a nonperturbative method, the QCD sum rules is a well established technique in the hadron physics since it is based on the fundamental QCD Lagrangian. In this work, we investigate the  $B(B_s) \rightarrow K_2^*(a_2, f_2)\ell\nu$  decays in the framework of the 3PSR method. For analysis of these decays, using the operator product expansion (OPE) in the deep Euclidean region and considering the contributions of the operators with dimension 3, 4 and 5, we calculate the transition form factors and consider their branching ratio values.

So far, the form factors of the semileptonic decays  $B(B_s) \rightarrow K_2^*(a_2, f_2)\ell\nu$  have been studied via the light cone QCD sum rules (LCSR) [10], the different approaches such as the perturbative QCD (PQCD) [5], the light-front quark model(LFQM) [11–13], and the ISGW II model [14]. However, the obtained results of these methods are different from each other. Any future experimental measurement on these form factors as well as decay rates and branching fractions and also their comparison with the results obtaining in the

theoretical works can give considerable information about the tensor meson properties.

The plan of the present paper is as follows: The 3PSR approach for calculation of the relevant form factors of the  $B(B_s) \rightarrow K_2^*(a_2, f_2)\ell\nu$  decays presented in Section II. The next Section is devoted to numeric results and discussions. In this part, the branching ratio values of the considered decays are reported. For a better analysis, the transition form factors and differential branching ratios related to these semileptonic decays are plotted with respect to the momentum transfer squared  $q^2$ . A comparison of our results for the form factor values in  $q^2 = 0$  and branching ratio data with predictions obtained from other approaches is also made in this section.

## II. THEORETICAL FRAMEWORK

In order to study of  $B(B_s) \rightarrow K_2^*(a_2, f_2)\ell\nu$  decays, we focus on the exclusive decay  $B_s \rightarrow K_2^*$  via the 3PSR. The  $B_s \rightarrow K_2^*\ell\nu$  decay governed by the tree level  $b \rightarrow u$  transition (see Fig. 1). In the framework of the 3PSR, the first step is appropriate definition of

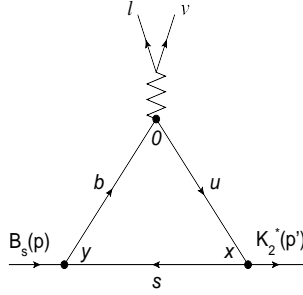


FIG. 1: Schematic picture of the spectator mechanism for the  $B_s \rightarrow K_2^*\ell\nu$  decay.

correlation function. In this work, the correlation function should be taken as

$$\Pi_{\alpha\beta\mu}(p^2, p'^2, q^2) = i \int \int d^4x d^4y e^{i(p'x - py)} \langle 0 | \mathcal{T} \left\{ j_{\alpha\beta}^{K_2^*}(x) j_\mu(0) j^{B_s}(y) \right\} | 0 \rangle, \quad (1)$$

where  $p$  and  $p'$  are four-momentum of the initial and final mesons, respectively.  $q^2$  is the squared momentum transfer and  $\mathcal{T}$  is the time ordering operator.  $j_\mu = \bar{u}\gamma_\mu(1 - \gamma_5)b$  is the transition current.  $j^{B_s}$  and  $j_{\alpha\beta}^{K_2^*}$  are also the interpolating currents of the  $B_s$  and the tensor meson  $K_2^*$ , respectively. With considering all quantum numbers, their interpolating currents can be written as

$$j^{B_s}(y) = \bar{b}(y)\gamma_5 s(y),$$

$$j_{\alpha\beta}^{K_2^*}(x) = \frac{i}{2} \left[ \bar{s}(x) \gamma_\alpha \overleftrightarrow{D}_\beta(x) u(x) + \bar{s}(x) \gamma_\beta \overleftrightarrow{D}_\alpha(x) u(x) \right], \quad (2)$$

where  $\overleftrightarrow{D}_\mu(x)$  denotes the four-derivative with respect to  $x$  acting simultaneously on the left and right. It is given as

$$\begin{aligned} \overleftrightarrow{D}_\mu(x) &= \frac{1}{2} \left[ \overrightarrow{D}_\mu(x) - \overleftarrow{D}_\mu(x) \right], \\ \overrightarrow{D}_\mu(x) &= \overrightarrow{\partial}_\mu(x) - i \frac{g}{2} \lambda^a \mathbf{A}_\mu^a(x), \\ \overleftarrow{D}_\mu(x) &= \overleftarrow{\partial}_\mu(x) + i \frac{g}{2} \lambda^a \mathbf{A}_\mu^a(x), \end{aligned}$$

where  $\lambda^a$  are the Gell-Mann matrices and  $\mathbf{A}_\mu^a(x)$  are the external gluon field.

The correlation function is a complex function of which the imaginary part comprises the computations of the phenomenology and real part comprises the computations of the theoretical part (QCD). By linking these two parts via the dispersion relation, the physical quantities are calculated. In the phenomenological part of the QCD sum rules approach, the correlation function in Eq. (1) is calculated by inserting two complete sets of intermediate states with the same quantum numbers as  $B_s$  and  $K_2^*$ . After performing four-integrals over  $x$  and  $y$ , it will be:

$$\Pi_{\alpha\beta\mu} = - \frac{\langle 0 | j_{\alpha\beta}^{K_2^*} | K_2^*(p') \rangle \langle K_2^*(p') | j_\mu | B_s(p) \rangle \langle B_s(p) | j^{B_s} | 0 \rangle}{(p^2 - m_{B_s}^2)(p'^2 - m_{K_2^*}^2)} + \text{higher states}. \quad (3)$$

In Eq. (3), the vacuum to initial and final meson state matrix elements are defined as

$$\langle 0 | j_{\alpha\beta}^{K_2^*} | K_2^*(p', \varepsilon) \rangle = f_{K_2^*} m_{K_2^*}^2 \varepsilon_{\alpha\beta}, \quad \langle 0 | j^{B_s} | B_s(p) \rangle = -i \frac{f_{B_s} m_{B_s}^2}{(m_b + m_s)}, \quad (4)$$

where  $f_{K_2^*}$  and  $f_{B_s}$  are the leptonic decay constants of  $K_2^*$  and  $B_s$  mesons, respectively.  $\varepsilon_{\alpha\beta}$  is polarization tensor of  $K_2^*$ . The transition current give a contribution to these matrix elements and it can be parametrized in terms of some form factors using the Lorentz invariance and parity conservation as follows:

$$\begin{aligned} c_V \langle K_2^*(p', \varepsilon) | \bar{u} \gamma_\mu (1 - \gamma_5) b | B_s(p) \rangle &= -i \varepsilon_\mu^* (m_{B_s} + m_{K_2^*}) A_1(q^2) + i (p + p')_\mu (\varepsilon^* \cdot q) \frac{A_2(q^2)}{m_{B_s} + m_{K_2^*}} \\ &\quad + i q_\mu (\varepsilon^* \cdot q) \frac{2m_{K_2^*}}{q^2} (A_3(q^2) - A_0(q^2)) + \epsilon_{\mu\nu\rho\sigma} \varepsilon^{*\nu} p^\rho p'^\sigma \frac{2V(q^2)}{m_{B_s} + m_{K_2^*}} \end{aligned} \quad (5)$$

$$\text{with } A_3(q^2) = \frac{m_{B_s} + m_{K_2^*}}{2m_{K_2^*}} A_1(q^2) - \frac{m_{B_s} - m_{K_2^*}}{2m_{K_2^*}} A_2(q^2) \text{ and } A_0(0) = A_3(0), \quad (6)$$

where  $q = p - p'$ ,  $P = p + p'$ , and  $\varepsilon_\mu^* = \frac{p_\lambda}{m_{B_s}} \varepsilon_{\mu\lambda}$ . The factor  $c_V$  accounts for the flavor content of particles:  $c_V = \sqrt{2}$  for  $a_2$ ,  $f_2$  and  $c_V = 1$  for  $K_2^*$  [18]. Inserting Eqs. (4) and (5) in Eq. (3) and performing summation over the polarization tensor as

$$\varepsilon_{\mu\nu} \varepsilon_{\alpha\beta} = \frac{1}{2} T_{\mu\alpha} T_{\nu\beta} + \frac{1}{2} T_{\mu\beta} T_{\nu\alpha} - \frac{1}{3} T_{\mu\nu} T_{\alpha\beta},$$

where  $T_{\mu\nu} = -g_{\mu\nu} + \frac{p'_\mu p'_\nu}{m_{K_2^*}^2}$ , the final representation of the physical side is obtained as

$$\begin{aligned} \Pi_{\alpha\beta\mu} = & \frac{f_{B_s} m_{B_s}}{(m_b + m_s)} \frac{f_{K_2^*} m_{K_2^*}^2}{(p^2 - m_{B_s}^2)(p'^2 - m_{K_2^*}^2)} \{ V'(q^2) i \epsilon_{\beta\mu\rho\sigma} p_\alpha p^\rho p'^\sigma + A'_0(q^2) p_\alpha p_\beta p'_\mu \\ & + A'_1(q^2) g_{\beta\mu} p_\alpha + A'_2(q^2) p_\alpha p_\beta p_\mu \} + \text{higher states}. \end{aligned} \quad (7)$$

For simplicity in calculations, the following redefinitions have been used in Eq. (7):

$$\begin{aligned} V'(q^2) &= \frac{V(q^2)}{m_{B_s} + m_{K_2^*}}, & A'_0(q^2) &= -\frac{m_{K_2^*}(A_3(q^2) - A_0(q^2))}{q^2}, \\ A'_1(q^2) &= -\frac{(m_{B_s} + m_{K_2^*})}{2} A_1(q^2), & A'_2(q^2) &= \frac{A_2(q^2)}{2(m_{B_s} + m_{K_2^*})}. \end{aligned}$$

Now, the QCD part of the correlation function is calculated by expanding it in terms of the OPE at large negative value of  $q^2$ :

$$\Pi_{\alpha\beta\mu} = C_{\alpha\beta\mu}^{(0)} \mathbf{I} + C_{\alpha\beta\mu}^{(3)} \langle 0 | \bar{\Psi} \Psi | 0 \rangle + C_{\alpha\beta\mu}^{(4)} \langle 0 | G_{\rho\nu}^a G_a^{\rho\nu} | 0 \rangle + C_{\alpha\beta\mu}^{(5)} \langle 0 | \bar{\Psi} \sigma_{\rho\nu} T^a G_a^{\rho\nu} \Psi | 0 \rangle + \dots, \quad (8)$$

where  $C_{\alpha\beta\mu}^{(i)}$  are the Wilson coefficients,  $\mathbf{I}$  is the unit operator,  $\bar{\Psi}$  is the local fermion field operator and  $G_{\rho\nu}^a$  is the gluon strength tensor. In Eq. (8) the first term is contribution of the perturbative and the other terms are contribution of the non-perturbative part.

To compute the portion of the perturbative part (Fig. 1), using the Feynman rules for the bare loop, we obtain:

$$\begin{aligned} C_{\alpha\beta\mu}^{(0)} = & -\frac{i}{4} \int \int d^4x d^4y e^{i(p'x - py)} \left\{ \text{Tr} \left[ S_s(x - y) \gamma_\alpha \overleftrightarrow{D}_\beta(x) S_u(-x) \gamma_\mu (1 - \gamma_5) S_b(y) \gamma_5 \right] \right. \\ & \left. + \text{Tr}[\alpha \leftrightarrow \beta] \right\}, \end{aligned} \quad (9)$$

taking the partial derivative with respect to  $x$  of the quark free propagators, and performing the Fourier transformation and using the Cutkosky rules, i.e.,  $\frac{1}{p^2 - m^2} \rightarrow -2i\pi \delta(p^2 - m^2)$ , imaginary part of the  $C_{\alpha\beta\mu}^{(0)}$  is calculated as

$$\begin{aligned} \text{Im} \left[ C_{\alpha\beta\mu}^{(0)} \right] = & \frac{1}{8\pi} \int d^4k \delta(k^2 - m_s^2) \delta((p + k)^2 - m_b^2) \delta((p' + k)^2 - m_u^2) (2k + p')_\beta \\ & \times \text{Tr}[(\not{k} + m_s) \gamma_\alpha (\not{p}' + \not{k} + m_u) \gamma_\mu (1 - \gamma_5) (\not{p} + \not{k} + m_b) \gamma_5] + \{\alpha \leftrightarrow \beta\}, \end{aligned} \quad (10)$$

where  $k$  is four-momentum of the spectator quark  $s$ . To solve the integral in Eq. (10), we will have to deal with the integrals such as  $I_0$ ,  $I_\alpha$ ,  $I_{\alpha\beta}$  and  $I_{\alpha\beta\mu}$  with respect to  $k$ . For example  $I_{\alpha\beta\mu}$  can be as:

$$I_{\alpha\beta\mu}(s, s', q^2) = \int d^4k [k_\alpha k_\beta k_\mu] \delta(k^2 - m_s^2) \delta((p+k)^2 - m_b^2) \delta((p'+k)^2 - m_u^2).$$

where  $s = p^2$  and  $s' = p'^2$ .  $I_0$ ,  $I_\alpha$ ,  $I_{\alpha\beta}$  and  $I_{\alpha\beta\mu}$  can be taken as an appropriate tensor structure as follows:

$$\begin{aligned} I_0 &= \frac{1}{4\sqrt{\lambda(s, s', q^2)}}, \\ I_\alpha &= B_1[p_\alpha] + B_2[p'_\alpha], \\ I_{\alpha\beta} &= D_1[g_{\alpha\beta}] + D_2[p_\alpha p_\beta] + D_3[p_\alpha p'_\beta + p'_\alpha p_\beta] + D_4[p'_\alpha p'_\beta], \\ I_{\alpha\beta\mu} &= E_1[g_{\alpha\beta} p_\mu + g_{\alpha\mu} p_\beta + g_{\beta\mu} p_\alpha] + E_2[g_{\alpha\beta} p'_\mu + g_{\alpha\mu} p'_\beta + g_{\beta\mu} p'_\alpha] + E_3[p_\alpha p_\beta p_\mu] \\ &\quad + E_4[p'_\alpha p_\beta p_\mu + p_\alpha p'_\beta p_\mu + p_\alpha p_\beta p'_\mu] + E_5[p'_\alpha p'_\beta p_\mu + p'_\alpha p_\beta p'_\mu + p_\alpha p'_\beta p'_\mu] \\ &\quad + E_6[p'_\alpha p'_\beta p'_\mu], \end{aligned} \quad (11)$$

The quantities  $\lambda(s, s', q^2)$ ,  $B_l$  ( $l = 1, 2$ ),  $D_j$  ( $j = 1, \dots, 4$ ), and  $E_r$  ( $r = 1, \dots, 6$ ), are indicated in the Appendix. Using the relations in Eq. (11),  $\text{Im}[C_{\alpha\beta\mu}^{(0)}]$  can be calculated for the each structure corresponding to Eq. (7) as follows:

$$\text{Im} \left[ C_{\alpha\beta\mu}^{(0)} \right] = \rho_V(i\epsilon_{\beta\mu\rho\sigma} p_\alpha p^\rho p'^\sigma) + \rho_0(p_\alpha p_\beta p'_\mu) + \rho_1(g_{\beta\mu} p_\alpha) + \rho_2(p_\alpha p_\beta p_\mu). \quad (12)$$

where the spectral densities  $\rho_i$ , ( $i = V, 0, 1, 2$ ) are found as

$$\begin{aligned} \rho_V(s, s', q^2) &= 24B_1\sqrt{\lambda} [B_1(m_s - m_b) + B_2(m_s - m_u) + m_s I_0], \\ \rho_0(s, s', q^2) &= 12[D_2(m_s - m_b) + D_3(m_s - m_u) + 2B_1 m_s - 2E_4(m_b - m_s)], \\ \rho_1(s, s', q^2) &= 3B_1[2m_s^2(m_b + m_u - m_s) - m_s(2m_b m_u + u) + \Delta(m_s - m_u) + \Delta'(m_s - m_b)] \\ &\quad + 6D_1(m_s - m_u) - 24E_1(m_b - m_s), \\ \rho_2(s, s', q^2) &= 24[D_2 m_s + E_3(m_s - m_b)]. \end{aligned}$$

Using the dispersion relation, the perturbative part contribution of the correlation function can be calculated as follows:

$$C_i^{(0)} = \int ds' \int ds \frac{\rho_i(s, s', q^2)}{(s - p^2)(s' - p'^2)}. \quad (13)$$

For calculation of the non-perturbative contributions (condensate terms), we consider the condensate terms of dimension 3, 4 and 5 related to the contributions of the quark-quark, gluon-gluon and quark-gluon condensate, respectively. They are more important than the other terms in the OPE. In the 3PSR, when the light quark is a spectator, the gluon-gluon condensate contributions can be easily ignored [19]. On the other hand, the quark condensate contributions of the light quark which is a non spectator, are zero after applying the double Borel transformation with respect to the both variables  $p^2$  and  $p'^2$ , because only one variable appears in the denominator. Therefore, only two important diagrams of dimension 3, 4 and 5 remain from the non-perturbative part contributions. The diagrams of these contributions corresponding to  $C_{\alpha\beta\mu}^{(3)}$  and  $C_{\alpha\beta\mu}^{(5)}$  are depicted in Fig. 2. After some calculations, the non-perturbative part of the correlation function are obtained

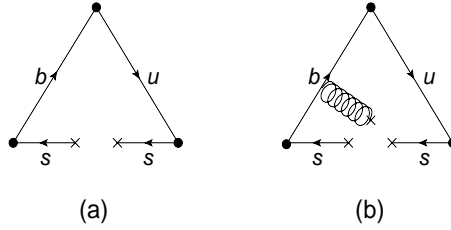


FIG. 2: The diagrams of the effective contributions of the condensate terms.

as follows:

$$\begin{aligned}
C_V^{(3)} + C_V^{(5)} &= -\frac{2\kappa}{(p^2 - m_b^2)^2(p'^2 - m_u^2)}, \\
C_0^{(3)} + C_0^{(5)} &= -\frac{4\kappa}{(p^2 - m_b^2)^2(p'^2 - m_u^2)}, \\
C_1^{(3)} + C_1^{(5)} &= \frac{\kappa}{(p^2 - m_b^2)(p'^2 - m_u^2)} + \frac{\kappa[(m_1 + m_2)^2 - q^2]}{(p^2 - m_b^2)^2(p'^2 - m_u^2)}, \\
C_2^{(3)} + C_2^{(5)} &= -\frac{4\kappa}{(p^2 - m_b^2)^2(p'^2 - m_u^2)},
\end{aligned} \tag{14}$$

where  $\kappa = \frac{(m_s^2 - m_0^2)}{48} \langle 0 | s\bar{s} | 0 \rangle$ ,  $m_0^2 = (0.8 \pm 0.2) \text{ GeV}^2$  [20], and  $\langle 0 | \bar{s}s | 0 \rangle = (0.8 \pm 0.2) \langle 0 | \bar{u}u | 0 \rangle$ ,  $\langle 0 | \bar{u}u | 0 \rangle = \langle 0 | \bar{d}d | 0 \rangle = -(0.240 \pm 0.010 \text{ GeV})^3$  that we choose the value of the condensates at a fixed renormalization scale of about 1 GeV.

To obtain sum rules for the form factors, the coefficients of the same structures from both sides of the correlation functions are matched. In order to suppress the contributions

of the higher states and continuum, the double Borel transformation is applied with respect to the initial and final momenta squared. So we have:

$$\begin{aligned}
V'(q^2) &= \frac{(m_b + m_s)e^{m_{B_s}^2/M_1^2}e^{m_{K_2^*}^2/M_2^2}}{f_{B_s}m_{B_s}f_{K_2^*}m_{K_2^*}^2} \left\{ \frac{-1}{(2\pi)^2} \int_{m_s^2}^{s_0'} ds' \int_{s_L}^{s_0} ds \rho_V(s, s', q^2) e^{-s/M_1^2} e^{-s'/M_2^2} \right. \\
&\quad \left. + \tilde{B} [C_V^{(3)} + C_V^{(5)}] \right\}, \\
A'_n(q^2) &= \frac{(m_b + m_s)e^{m_{B_s}^2/M_1^2}e^{m_{K_2^*}^2/M_2^2}}{f_{B_s}m_{B_s}f_{K_2^*}m_{K_2^*}^2} \left\{ \frac{-1}{(2\pi)^2} \int_{m_s^2}^{s_0'} ds' \int_{s_L}^{s_0} ds \rho_n(s, s', q^2) e^{-s/M_1^2} e^{-s'/M_2^2} \right. \\
&\quad \left. + \tilde{B} [C_n^{(3)} + C_n^{(5)}] \right\}, \tag{15}
\end{aligned}$$

where  $n = 0, \dots, 2$ ,  $s_0$  and  $s_0'$  are the continuum thresholds in the initial and final channels, respectively. The lower limit in the integration over  $s$  is:  $s_L = m_b^2 + \frac{m_b^2}{m_b^2 - q^2} s'$ . Also  $\tilde{B}$  transformation is defined as follows:

$$\tilde{B} \left[ \frac{1}{(p^2 - m_b^2)^m (p'^2 - m_u^2)^n} \right] = \frac{(-1)^{m+n}}{\Gamma(n)\Gamma(m)} \frac{e^{-m_b^2/M_1^2} e^{-m_u^2/M_2^2}}{(M_1^2)^{m-1} (M_2^2)^{n-1}}, \tag{16}$$

where  $M_1^2$  and  $M_2^2$  are Borel mass parameters.

We would like to provide the same results for the  $B \rightarrow a_2 \ell \nu$ , and  $B \rightarrow f_2 \ell \nu$  decays. With a little bit of change in the above expressions such as  $s \leftrightarrow d(u)$  and  $m_{K_2^*} \leftrightarrow m_{a_2}(m_{f_2})$ , we can easily find similar results in Eq. (15) for the form factors of the new transitions.

### III. NUMERICAL ANALYSIS

In this section, we numerically analyze the sum rules for the form factors  $V(q^2)$ ,  $A_0(q^2)$ ,  $A_1(q^2)$  and  $A_2(q^2)$  as well as branching ratio values of the transitions  $B(B_s) \rightarrow T$ , where  $T$  can be one of the tensor mesons  $K_2^*$ ,  $a_2$ , or  $f_2$ . The values of the meson masses and leptonic decay constants are chosen as presented in Table I. Also  $m_b = 4.820$  GeV,  $m_s = 0.150$  GeV

TABLE I: The values of the meson masses [22] and decay constants [5] in GeV.

meson	$B_s$	$B$	$K_2^*$	$a_2$	$f_2$
Mass	5.366	5.279	1.425	1.318	1.275
Decay Constant	0.230	0.190	0.118	0.107	0.102

[21],  $m_\tau = 1.776$  GeV, and  $m_\mu = 0.105$  GeV [22].



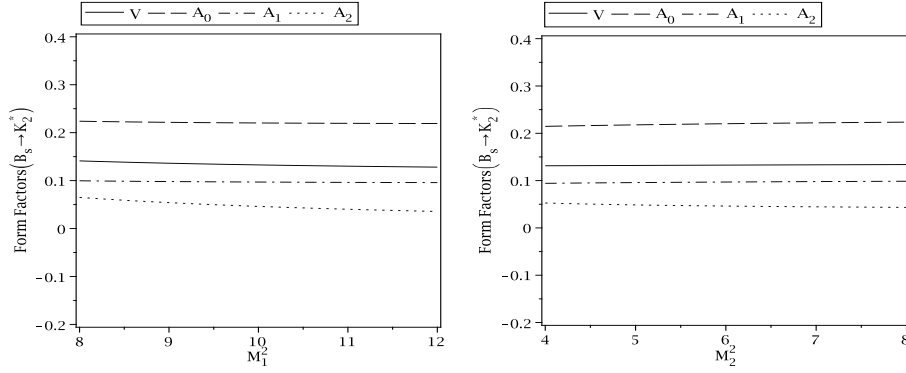


FIG. 3: The form factors of  $B_s \rightarrow K_2^*$  on  $M_1^2$  and  $M_2^2$ .

From the 3PSR for the form factors, it is clear that they also contain four auxiliary parameters, namely the continuum thresholds  $s_0$  and  $s'_0$  and the Borel mass parameters  $M_1^2$  and  $M_2^2$  as the main input. These are not physical quantities, hence the form factors, should be independent of these parameters. The continuum thresholds,  $s_0$  and  $s'_0$  are not completely arbitrary, but these are in correlation with the energy of the first excited state with the same quantum numbers as the considered interpolating currents. The value of the continuum threshold  $s_0^{B(B_s)} = 35 \text{ GeV}^2$  [23] calculated from the 3PSR. The values of the continuum threshold  $s'_0$  for the tensor mesons  $K_2^*$ ,  $a_2$  and  $f_2$  are taken to be  $s_0^{K_2^*} = 3.13 \text{ GeV}^2$ ,  $s_0^{a_2} = 2.70 \text{ GeV}^2$  and  $s_0^{f_2} = 2.53 \text{ GeV}^2$ , respectively [9].

We search for the intervals of the Borel mass parameters so that our results are almost insensitive to their variations. One more condition for the intervals of these parameters is the fact that the aforementioned intervals must suppress the higher states, continuum and contributions of the highest-order operators. In other words, the sum rules for the form factors must converge. As a result, we get  $8 \text{ GeV}^2 \leq M_1^2 \leq 12 \text{ GeV}^2$  and  $4 \text{ GeV}^2 \leq M_2^2 \leq 8 \text{ GeV}^2$ . To show how the form factors depend on the Borel mass parameters, as examples, we depict the variations of the form factors  $V$ ,  $A_0$ ,  $A_1$  and  $A_2$  for  $B_s \rightarrow K_2^* \ell \nu$  at  $q^2 = 0$  with respect to the variations of the  $M_1^2$  and  $M_2^2$  parameters in their working regions in Fig. 3. From these figures, it revealed that the form factors weakly depend on these parameters in their working regions.

Using the working regions for the continuum thresholds and Borel mass parameters as well as other input parameters, we proceed to find the behavior of the form factors in terms of  $q^2$ . We calculated the  $q^2$  dependence of the form factors in the region where the sum rule

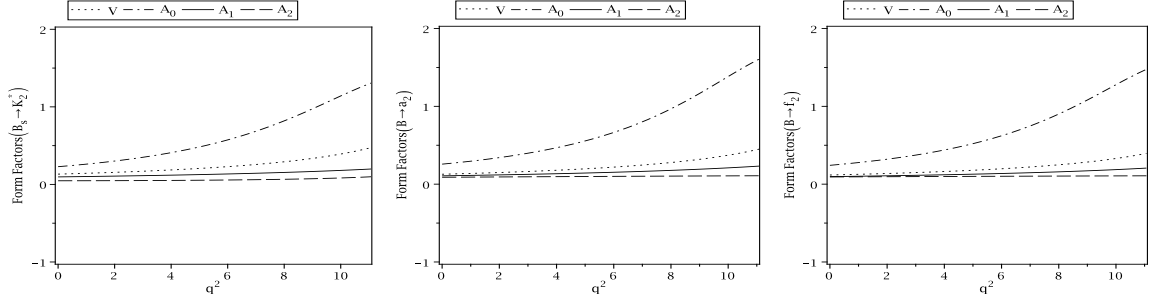


FIG. 4: The SR predictions for the form factors of the  $B(B_s) \rightarrow T\ell\nu$  transitions on  $q^2$ .

is valid, i.e.,  $0 \leq q^2 \leq 11 \text{ GeV}^2$ . The dependence of the form factors  $V$ ,  $A_0$ ,  $A_1$  and  $A_2$  on  $q^2$  for  $B \rightarrow T$  transitions are shown in Fig. 4. In order to estimate the decay width of the  $B(B_s) \rightarrow T\ell\nu$  transition, we have to obtain their fit functions in the whole physical region,  $0 \leq q^2 \leq (m_{B(B_s)} - m_T)^2$ . We find that the sum rules predictions for the form factors are well fitted to the following function:

$$f(q^2) = \frac{f(0)}{1 - a(\frac{q^2}{m_{B(B_s)}^2}) + b(\frac{q^2}{m_{B(B_s)}^2})^2}. \quad (17)$$

The values of the parameters  $f(0)$ ,  $a$ , and  $b$  for the transition form factors of the  $B \rightarrow T$  are given in the Table II.

TABLE II: Parameter values appearing in the fit functions of the  $B \rightarrow T\ell\nu$  decays.

Form Factor	$f(0)$	$a$	$b$	Form Factor	$f(0)$	$a$	$b$
$V^{B_s \rightarrow K_2^*}$	0.13	2.19	0.83	$A_0^{B_s \rightarrow K_2^*}$	0.23	3.77	4.21
$A_1^{B_s \rightarrow K_2^*}$	0.10	1.36	0.09	$A_2^{B_s \rightarrow K_2^*}$	0.05	0.21	-2.99
$V^{B \rightarrow a_2}$	0.13	2.10	0.75	$A_0^{B \rightarrow a_2}$	0.26	3.71	4.03
$A_1^{B \rightarrow a_2}$	0.11	1.45	0.23	$A_2^{B \rightarrow a_2}$	0.09	0.63	0.46
$V^{B \rightarrow f_2}$	0.12	2.01	0.60	$A_0^{B \rightarrow f_2}$	0.24	3.70	4.02
$A_1^{B \rightarrow f_2}$	0.10	1.40	0.16	$A_2^{B \rightarrow f_2}$	0.09	0.46	0.29

In Table III, our results for the form factors of  $B \rightarrow T\ell\nu$  decays in  $q^2 = 0$  is compared with those of other approaches such as the LCSR, the PQCD, the LFQM, and the ISGW II model. From this table, results for all form factors from the ISGW II model possess a mines sign in contrast with this work, the LCSR and the PQCD where all those have a

TABLE III: Comparison of the form factor values of the  $B \rightarrow T\ell\nu$  decays in  $q^2 = 0$  in different approaches.

Form Factor	This Work	LCSR[10]	PQCD[5]	ISGW[14]	LFQM[11–13]
$V^{B_s \rightarrow K_2^*}$	$0.13 \pm 0.03$	0.15	0.18	—	—
$A_0^{B_s \rightarrow K_2^*}$	$0.23 \pm 0.06$	0.22	0.15	-0.27	—
$A_1^{B_s \rightarrow K_2^*}$	$0.10 \pm 0.02$	0.12	0.11	-0.39	—
$A_2^{B_s \rightarrow K_2^*}$	$0.05 \pm 0.01$	0.05	0.07	-0.47	—
$V^{B \rightarrow a_2}$	$0.13 \pm 0.03$	0.18	0.18	—	-0.28
$A_0^{B \rightarrow a_2}$	$0.26 \pm 0.07$	0.21	0.18	-0.18	0.20
$A_1^{B \rightarrow a_2}$	$0.11 \pm 0.04$	0.14	0.11	-0.35	-0.03
$A_2^{B \rightarrow a_2}$	$0.09 \pm 0.02$	0.09	0.06	-0.45	-0.17
$V^{B \rightarrow f_2}$	$0.12 \pm 0.04$	0.18	0.12	—	—
$A_0^{B \rightarrow f_2}$	$0.24 \pm 0.06$	0.20	0.13	-0.08	—
$A_1^{B \rightarrow f_2}$	$0.10 \pm 0.02$	0.14	0.08	-0.24	—
$A_2^{B \rightarrow f_2}$	$0.09 \pm 0.02$	0.10	0.04	-0.34	—

positive sign. Our results are in good agreement with those of the LCSR and PQCD in all cases.

Now, we proceed to calculate the decay width and branching ratio of the process under consideration. The differential decay width for  $B \rightarrow T\ell\nu$  transition is obtained as:

$$\frac{d\Gamma(B \rightarrow T\ell\nu)}{dq^2} = \frac{|G_F V_{ub}|^2 \sqrt{\lambda(m_B^2, m_T^2, q^2)}}{256 m_B^3 \pi^3 q^2} \left(1 - \frac{m_\ell^2}{q^2}\right)^2 (X_L + X_+ + X_-), \quad (18)$$

$m_\ell$  represents the mass of the charged lepton. The other parameters are defined as

$$\begin{aligned} X_L &= \frac{1}{9} \frac{\lambda}{m_T^2 m_B^2} [(2q^2 + m_\ell^2) h_0^2(q^2) + 3\lambda m_\ell^2 A_0^2(q^2)], \\ X_\pm &= \frac{2q^2}{3} (2q^2 + m_\ell^2) \frac{\lambda}{8m_T^2 m_B^2} [(m_B + m_T) A_1(q^2) \mp \frac{\sqrt{\lambda}}{m_B + m_T} V(q^2)]^2, \\ h_0(q^2) &= \frac{1}{2m_T} [(m_B^2 - m_T^2 - q^2)(m_B + m_T) A_1(q^2) - \frac{\lambda}{m_B + m_T} A_2(q^2)]. \end{aligned}$$

Integrating Eq. (18) over  $q^2$  in the whole physical region, and using  $V_{ub} = (3.89 \pm 0.44) \times 10^{-3}$  [22], the branching ratios of the  $B \rightarrow T\ell\nu$  are obtained. The differential branching

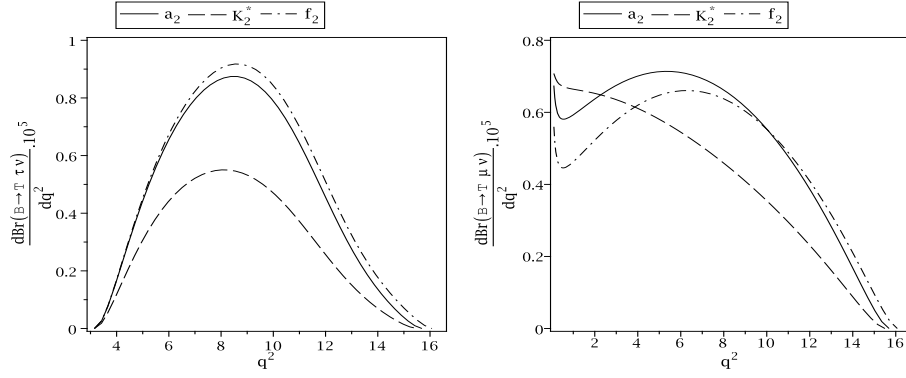


FIG. 5: The differential branching ratios of the semileptonic  $B \rightarrow T\ell\nu$  decays on  $q^2$ .

ratios of the  $B \rightarrow T\ell\nu$  decays on  $q^2$  are shown in Fig. 5. The branching ratio values of these decays are also obtained as presented in Table IV. Furthermore, this table contains the results estimated via the PQCD. Considering the uncertainties, our estimations for the branching ratio values of the  $B \rightarrow T\ell\nu$  decays are in consistent agreement with those of the PQCD.

TABLE IV: Comparison of the branching ratio values of the  $B \rightarrow T\ell\nu$  decays with those of the PQCD (in units of  $10^{-4}$ ).

	This Work	PQCD[5]
$\text{Br}(B \rightarrow a_2\mu\nu)$	$0.82 \pm 0.25$	1.16
$\text{Br}(B_s \rightarrow K_2^*\mu\nu)$	$0.65 \pm 0.20$	0.73
$\text{Br}(B \rightarrow f_2\mu\nu)$	$0.77 \pm 0.23$	0.69
$\text{Br}(B \rightarrow a_2\tau\nu)$	$0.51 \pm 0.17$	0.41
$\text{Br}(B_s \rightarrow K_2^*\tau\nu)$	$0.35 \pm 0.11$	0.25
$\text{Br}(B \rightarrow f_2\tau\nu)$	$0.53 \pm 0.18$	0.25

In summary, we considered the  $B_s(B) \rightarrow K_2^*(a_2, f_2)\ell\nu$  channels and computed the relevant form factors considering the contribution of the quark condensate corrections. Our results are in good agreement with those of the LCSR and PQCD in all cases. We also evaluated the total decays widths and the branching ratios of these decays. Our branching ratio values of these decays are in consistent agreement with those of the PQCD.

## **Acknowledgments**

Partial support of Isfahan university of technology research council is appreciated.

## Appendix

In this appendix, the explicit expressions of the coefficients  $\lambda(s, s', q^2)$ ,  $B_l$  ( $l = 1, 2$ ),  $D_j$  ( $j = 1, \dots, 4$ ), and  $E_r$  ( $r = 1, \dots, 6$ ), are given.

$$\lambda(s, s', q^2) = s^2 + s'^2 + (q^2)^2 - 2sq^2 - 2s'q^2 - 2ss',$$

$$B_1 = \frac{I_0}{\lambda(s, s', q^2)} [2s'\Delta - \Delta'u],$$

$$B_2 = \frac{I_0}{\lambda(s, s', q^2)} [2s\Delta' - \Delta u],$$

$$D_1 = -\frac{I_0}{2\lambda(s, s', q^2)} [4ss'm_s^2 - s\Delta'^2 - s'\Delta^2 - u^2m_s^2 + u\Delta\Delta'],$$

$$D_2 = -\frac{I_0}{\lambda^2(s, s', q^2)} [8ss'^2m_s^2 - 2ss'\Delta' - 6s'^2\Delta^2 - 2u^2s'm_s^2 + 6s'u\Delta\Delta' - u^2\Delta'^2],$$

$$D_3 = \frac{I_0}{\lambda^2(s, s', q^2)} [4ss'um_s^2 + 4ss'\Delta\Delta' - 3su\Delta'^2 - 3u\Delta^2s' - u^3m_s^2 + 2u^2\Delta\Delta'],$$

$$D_4 = \frac{I_0}{\lambda^2(s, s', q^2)} [-6s'u\Delta\Delta' + 6s^2\Delta'^2 - 8s^2s'm_s^2 + 2u^2s'm_s^2 + u^2\Delta^2 + 2ss'\Delta^2],$$

$$E_1 = \frac{I_0}{2\lambda^2(s, s', q^2)} [8s'^2m_s^2\Delta s - 2s'm_s^2\Delta u^2 - 4um_s^2\Delta'ss' + u^3m_s^2\Delta' - 2s'^2\Delta^3 \\ + 3s'u\Delta^2\Delta' - 2\Delta'^2\Delta ss' - \Delta'^2\Delta u^2 + us\Delta^3],$$

$$E_2 = \frac{I_0}{2\lambda^2(s, s', q^2)} [8s^2m_s^2\Delta's' - 2s^2\Delta'^3 - 4um_s^2\Delta ss' - 2\Delta^2\Delta'ss' + 3us\Delta'^2\Delta \\ - 2sm_s^2\Delta'u^2 + s'u\Delta^3 + u^3m_s^2\Delta - \Delta^2\Delta'u^2],$$

$$E_3 = -\frac{I_0}{\lambda^3(s, s', q^2)} [48sm_s^2\Delta s'^3 - 24ss'^2um_s^2\Delta' - 12ss'^2\Delta'^2\Delta + 6su\Delta'^3s' - 20s'^3\Delta^3 \\ + 30s'^2u\Delta^2\Delta' - 12s'^2m_s^2\Delta u^2 - 12s'\Delta'^2\Delta u^2 + 6s'u^3m_s^2\Delta' + u^3\Delta'^3],$$

$$E_4 = -\frac{I_0}{\lambda^3(s, s', q^2)} [16s^2m_s^2\Delta's'^2 - 4s^2\Delta'^3s' - 12ss'^2\Delta^2\Delta' - 24ss'^2um_s^2\Delta + 3u^3\Delta'^2\Delta \\ + 18su\Delta'^2\Delta s' - 4s\Delta'^3u^2 + 10s'^2u\Delta^3 + 6s'u^3m_s^2\Delta - 12s'\Delta^2\Delta'u^2 - 2m_s^2\Delta'u^4 \\ + 4ss'u^2m_s^2\Delta'],$$

$$E_5 = -\frac{I_0}{\lambda^3(s, s', q^2)} [16s^2m_s^2\Delta s'^2 - 24s^2s'um_s^2\Delta' - 12s^2s'\Delta'^2\Delta + 10us^2\Delta'^3 - 4ss'^2\Delta^3 \\ + 4ss'u^2m_s^2\Delta + 18su\Delta^2\Delta's' + 6su^3m_s^2\Delta' - 12s\Delta^2\Delta u^2 - 4s'\Delta^3u^2 - 2m_s^2\Delta u^4 \\ + 3u^3\Delta^2\Delta'],$$

$$E_6 = -\frac{I_0}{\lambda^3(s, s', q^2)} [48s^3m_s^2\Delta's' - 20s^3\Delta'^3 - 12s^2\Delta^2\Delta's' - 24s^2s'um_s^2\Delta - 12s^2m_s^2\Delta'u^2 \\ + 30us^2\Delta'^2\Delta + 6su\Delta^3s' - 12s\Delta^2\Delta'u^2 + 6su^3m_s^2\Delta + u^3\Delta^3],$$

$$\Delta = s + m_s^2 - m_b^2, \quad \Delta' = s' + m_s^2 - m_u^2, \quad u = s + s' - q^2.$$

- 
- [1] B. Aubert et al., BABAR Collaboration, Phys. Rev. D 79, 052005 (2009)
  - [2] B. Aubert et al., BABAR Collaboration, Phys. Rev. Lett. 101, 161801 (2008).
  - [3] B. Aubert et al., BABAR Collaboration, Phys. Rev. D 78, 092008 (2008).
  - [4] E. Barberio et al., Heavy Flavor Averaging Group (HFAG), arXiv: 0808.1297.
  - [5] W. Wang, Phys. Rev. D 83, 014008 (2011).
  - [6] S. V. Dombrowski, Nucl. Phys. Proc. Suppl. 56, 125 (1997).
  - [7] C. Amsler et al., Particle Data Group, Phys. Lett. B 667, 1 (2008).
  - [8] D. M. Li, H. Yu, and Q. X. Shen, J. Phys. G 27, 807 (2001).
  - [9] H. Y. Cheng, Y. Koike, and K. C. Yang, Phys. Rev. D 82, 054019 (2010).
  - [10] K. C. Yang, Phys. Lett. B 695, 444 (2011).
  - [11] H. Y. Cheng, C. K. Chua and C. W. Hwang, Phys. Rev. D 69, 074025 (2004).
  - [12] H. Y. Cheng and C. K. Chua, Phys. Rev. D 69, 094007 (2004) [Erratum-ibid. D 81, 059901 (2010)].
  - [13] H. Y. Cheng and C. K. Chua, Phys. Rev. D 81, 114006 (2010).
  - [14] N. Sharma and R. C. Verma, Phys. Rev. D 82, 094014 (2010).
  - [15] P. Colangelo, F. De Fazio, P. Santorelli and E. Scrimieri, Phys. Rev. D 53, 3672 (1996).
  - [16] M. Z. Yang, Phys. Rev. D 73, 034027 (2006).
  - [17] N. Gharamany and R. Khosravi, Phys. Rev. D 80, 016009 (2009).
  - [18] P. Ball, R. Zwicky, Phys. Rev. D 71, 014029 (2005).
  - [19] P. Colangelo and A. Khodjamirian, arXiv: hep-ph/0010175; A. V. Radyushkin, arXiv: hep-ph/0101227.
  - [20] P. Colangelo and A. Khodjamirian, in *At the Frontier of Particle Physics/Handbook of QCD*, edited by M. Shifman (World Scientific, Singapore, 2001), Vol. III, p. 1495.
  - [21] M. Q. Huang, Phys. Rev. C 69, 114015 (2004).
  - [22] J. Beringer et al., Particle Data Group, Phys. Rev. D 86, 010001 (2012).
  - [23] M. A. Shifman, A. I. Vainshtein and V. I. Zakharov, Nucl. Phys. B 147, 385, (1979)
  - [24] Z. Guo, S. Narison, J. M. Richard and Q. Zhao, Phys. Rev. D 85, 114007 (2012).
  - [25] R. Khosravi and M. Janbazi, Phys. Rev. D 87, 016003 (2013).

[26] R. Khosravi and M. Janbazi, Phys, Rev, D 89, 016001 (2014).